Investigations of stacking faults in stacked granular perpendicular recording media with a high anisotropy CoPt layer

Y. Yang, B. Varghese, H.K. Tan, S. K. Wong, and S.N. Piramanayagam*, Senior Member, IEEE,

Data Storage Institute, A*STAR (Agency for Science, Technology and Research), Singapore 117608

Microstructural investigations of granular perpendicular recording media based on stacked CoPt-alloy layers were carried out using high resolution transmission electron microscopy (HRTEM). In the structure investigated, a thin layer of CoPt with high Pt concentration was inserted in order to meet the thermal stability requirements at higher densities. The increase in the coercivity and nucleation field of the sample observed for the insertion of a thin layer of CoPt (3 nm), and the decrease beyond this critical thickness has been explained based on HRTEM studies. HRTEM results indicated that the insertion of thicker CoPt layer causes stacking faults and the presence of fcc phase in the CoCrPt layers on the top. The number of stacking faults and the fcc-content in grains depends on the thickness of CoPt layer, indicating that the observed changes in magnetic properties arise due to the microstructural changes.

***Index Terms*—perpendicular magnetic recording, transmission electron microscopy, stacking faults, magnetic recording media**

I. Introduction

GRANULAR perpendicular recording media technology based on stacked layer of CoCrPt alloys with oxide grain boundaries has the potential to extend the media trilemma to areal densities above 1 Terabits per square inch (Tbpsi) [1-5]. Shingled magnetic recording is expected to aid in areal densities higher than 1 Tbpsi. Alternatively, disk drives filled with helium gas are also considered for achieving high capacities in hard disk drives (HDD). The current recording media have a graded anisotropy in order to extend the media trilemma issues [4-7] In order to achieve thermally stable grains at higher densities, materials with higher anisotropy are deposited at the bottom of the stack [6-8]. The layers at the top are made of relatively lower anisotropy, enabling a writing process that leads to a cascade of magnetization reversal from top to bottom [3-8]. CoPt alloys with a higher anisotropy are required for the bottom layer. $L1_0$ ordered CoPt has a high anisotropy [9]. However, the anisotropy field of this media is so high that it requires heat-assisted magnetic recording technology. Moreover, it requires a totally different set of layer design and solutions for microstructure control. $L1_1$ ordered CoPt, which can be grown hetero-epitaxially on the seedlayers of perpendicular media, has been demonstrated to show high anisotropy. However, high coercivity media with suitable segregants have not been demonstrated yet [10-12]. Therefore, CoPt alloys in hcp phase that could segregate into a granular structure while maintaining a high anisotropy are desirable materials [13].

The simplest way to increase the anisotropy of the hcp-based CoPt alloy layers is to increase the Pt concentration. However, Pt concentration in excess of 30 at% has been reported to lead to a reduction in the anisotropy due to stacking faults and to the formation of fcc phase [14,15]. In hard disk media, the Pt concentration is kept typically below 20 at%, in order to achieve stable hcp phase and to avoid stacking faults and the higher cost associated with Pt. Recently, we have reported that thin layers (about 3 nm) of near-equiatomic CoPt, even with Pt composition as high as 55 at%, can be prepared without stacking faults [16]. Beyond 3 nm, stacking faults and fcc-phased CoPt were formed, resulting in a reduced anisotropy. In those samples, a higher deposition temperature and thicker seedlayers of Ru were used. In this paper, we investigate the effect of inserting a near-equiatomic CoPt layer at room temperature in granular media using high resolution transmission electron microscopy (HRTEM). The stacking faults and the formation of fcc-CoPt alloy, which are induced by CoPt with excessive Pt, are studied in significant detail.

II. Experimental Details

Intevac Lean 200B production type sputtering tool was used for making samples of this study. Typical amorphous CoTaZr-alloy soft underlayers and seedlayers based on NiW/Ru were deposited on glass substrate prior to the deposition of the magnetic layer. The first ruthenium layer (Ru_1) and the second ruthenium layers (Ru_2), which are required to provide the necessary crystallographic texture and segregation, were sputtered at Ar gas pressures of 0.5 Pa and 5 Pa respectively. Figure 1(a) shows the schematic illustration of the samples made under this study. The main recording layer thickness was maintained at 10 nm in all the samples and the thickness of inserted CoPt layer was varied from 0 to 6 nm. The magnetic layers, except the capping layer, were also sputtered at 5 Pa. The samples were characterized using alternating gradient force magnetometry (AGFM), transmission electron microscopy (TEM), and magneto-optic Kerr Effect (MOKE).

III. RESULTS

1) Magnetic Properties

Fig. 1(b) shows the hysteresis loops of the samples in this study. It can be noticed that the coercivity (H_c) and the nucleation field (H_n) of the sample without CoPt is about 4.5 kOe and 1.5 kOe respectively. With the addition of 3 nm CoPt layer below CoCrPt-oxide layer, the coercivity and the nucleation field increases. Further increase of CoPt thickness reduces H_c and H_n.

The increase of H_c and H_n with 3 nm is expected to be due to the increase of K_uV, where K_u is the anisotropy constant and V is the volume of the grain. The increase in K_uV could be due

to a few possibilities; increased K_u due to the CoPt layer, increased V due to the insertion of 3 nm thick layer of CoPt or both. Time-dependent coercivity measurements indicated that the K_uV/k_BT increased from a value of 59 in sample with no CoPt to 82 in samples with 3 nm CoPt. Simple calculations indicated that the increase of V alone cannot account for such a large increase in K_uV/k_BT. The average K_u of the 3 nm thick CoPt layer was estimated to be at least 35% larger than that of the CoCrPt:oxide layer.

When the thickness of CoPt is increased beyond 3 nm, H_c and H_n decreases despite the increase of V. Therefore, it is expected that the K_u is reduced. It may be argued that the CoPt layer was deposited without any segregant material and it is likely that thicker CoPt layer increases the exchange coupling, resulting in a reduction in the coercivity. The increase in the slope of hysteresis loops as a function of CoPt thickness indicates the possibility of such an increase in exchange coupling. However, the tremendous reduction in the value of H_n (from about 2300 Oe in 3 nm CoPt samples to about 1700 in 6 nm CoPt samples) cannot be accounted for by the increase of exchange coupling alone. It is most likely due to a decrease of anisotropy constant of CoPt layer. K_uV/k_BT of the sample with 6 nm CoPt layer was 89, only 8% larger than that of sample with 3 nm CoPt despite an increase in thickness by 100%. Simple calculations based on the K_uV/k_BT data indicate that the K_u of the 6 nm CoPt is reduced by about 20%. Several reports, in the past, have reported such a reduction in anisotropy with high Pt concentration. In most of those studies, the anisotropy was measured in samples with thickness above 10 nm [14,15].

2) TEM investigations

In order to understand if the reduction in the H_n values of the samples is caused by a reduction in anisotropy constant of CoPt, due to the possibility of stacking faults and the presence of low-anisotropy fcc phase, detailed TEM analyses were carried out using an FEI Tecnai X-TWIN operated at 200 kV. HRTEM images were taken from cross-section of the samples with incident beam along the $[2\bar{1}\bar{1}0]_{hcp}$ ($[011]_{fcc}$) direction with respect to the individual CoPt/CoCrPt grains, which ensures that the stacking faults are clearly visible when present [17]. HRTEM is helpful to understand the origin of inferior magnetic properties in samples with thicker CoPt. Recently, we have observed a 2-3 nm epitaxial grown hcp phase of near-equiatomic CoPt on Ru layer using HRTEM [18]. Stacking faults and phase transformation from hcp to fcc were observed, and the lower anisotropy in thicker samples was attributed to increased thickness of fcc phase. We extend those investigations on a sample set that is closer to commercial hard disk media and correlate the thickness dependent magnetic properties with the microstructure of CoPt and CoCrPt layers.

Figures 2 (a-c) show typical cross-sectional TEM images of samples with CoPt thickness of 3, 4.5, and 6 nm, respectively. It can be noticed that there are streaks in the grains of CoCrPt layers, indicating the presence of stacking faults in all the samples. The streaks are stacking faults which can be detected by diffraction contrast image at low magnification, corresponding to planar faults on (111) planes when the incident beam direction is [011]. A general trend can be observed that the intensity of stacking faults for a given number of grains is larger for the sample with 4.5 and 6 nm CoPt layer. However, phase information (whether the crystal is fcc or hcp) is missing from diffraction contrast images. Hence, HRTEM investigations are necessary to confirm the microstructure and the presence of stacking faults.

Figures 3 (a, f and g) show the representative cross-sectional HRTEM analysis of three samples with the CoPt thickness of 3, 4.5, and 6 nm, respectively. The measured layer thickness for CoCrPt and CoPt layers are within the targeted thickness. Detailed structural analysis by fast Fourier transformed patterns (FFTs) are shown in Figures 3 (b-e), which confirms the existence of both fcc and hcp phases in the CoPt and CoCrPt layers. As shown in Figure 3 (a), the hcp phase of CoPt has a thickness slightly less than 3 nm followed by a more stable fcc phase. Similar phase transformation of the inserted near-equiatomic CoPt from metastable hcp phase to fcc phase has been observed in our previous work [15]. An fcc phase with thickness less than 2 nm could be observed at the CoCrPt/CoPt interface, which is likely to be induced by epitaxial growth of CoCrPt on top of $CoPt_{fcc}$. Phase transformations from hcp to fcc and vice versa are indicated by $(\bar{1}1\bar{1})_{fcc}$ (blue lines) and $(0\bar{1}11)_{hcp}$ planes (green lines) [18] for a clearer view. These two planes have an intersection angle of $9.14°$ or $131.9°$ if the fcc phase grain is in a mirror reflection relative to former one, and thus can be easily distinguished. From Ru to $CoPt_{hcp}$, the epitaxial relationship follows Ru $(0001)_{hcp}\langle 2\bar{1}\bar{1}0\rangle_{hcp}$//CoPt $(0001)_{hcp}\langle 2\bar{1}\bar{1}0\rangle_{hcp}$, and from $CoPt_{fcc}$ to $CoPt_{hcp}$ or vice versa, the epitaxial relationship follows CoPt $(11\bar{1})_{fcc}\langle 011\rangle_{fcc}$//CoPt $(0001)_{hcp}\langle 2\bar{1}\bar{1}0\rangle_{hcp}$. In this study, the CoCrPt continued to follow the fcc structure of CoPt for another 1-3 nm, and transformed to a more stable hcp phase. Significant increase in the thickness of the metastable $CoCrPt_{fcc}$ can be observed in samples with 4.5 and 6 nm CoPt. The total fcc phase thickness at the CoCrPt/CoPt interface found in Figures 3 (f, g, and h) is 1.3, 3.0, and 4.9 nm, for inserted CoPt thickness of 3, 4.5, and 6 nm, respectively. Twinning structure of fcc phase could also be observed in Figure 3 (h) for the 6 nm CoPt sample.

It can be noticed that the CoCrPt layer shows stacking faults and fcc phased layers, which leads to a drop in the anisotropy constant. The trend of H_c and H_n of the media as a function of thickness of CoPt (Figure 1(b)) can be understood by studying the number of stacking faults per grain found in CoCrPt layer. As shown in Figures 3 (f, g, and h), the HRTEM clearly shows the phase transformation within CoCrPt layer, which are indicated by $(\bar{1}1\bar{1})_{fcc}$ and $(0\bar{1}11)_{hcp}$ planes using blue and green lines, respectively. In these samples, both phase transformation and stacking faults are exists. To make this simple, we count as one stacking fault when the phase transforms from hcp to fcc and transforms back to hcp, which corresponds to the streaks observed in low magnification TEM. The sample with 3 nm CoPt insertion layer shows significantly lower number of stacking faults and fcc phase in the CoCrPt, which is also less than that in the sample without CoPt. As the thickness of CoPt increases, the amount of

stacking faults also increases, which could be induced by thicker fcc phase at the CoCrPt/CoPt interface. The content of fcc phase in the CoCrPt grain also increases as more stacking faults appear. The fcc content in the CoCrPt grain is estimated to be 12.9%, 48.5%, and 64.5% for CoPt thickness of 3, 4.5, and 6 nm, respectively.

The trend of fcc-content and the number of stacking faults is shown in figure 4 as a function of CoPt thickness. A close to linear relationship between the average number of stacking faults and the CoPt thickness is shown in Figure 4. The average number of stack faults is found by sampling at least 5 grains per sample, which is 2.2, 3.1, and 4 for CoPt thickness of 3, 4.5, and 6 nm, respectively. Observation of more stacking faults with an increase of CoPt thickness correlates well with the change of H_n and H_c for samples containing thicker CoPt layers. The fcc content in the film also increases with thickness, indicating that the increase in stacking faults and the fcc-content is the reason for the reduction of H_n and H_c for samples containing thicker CoPt layers.

There are several causes for stacking faults in CoPt-based media thin films, such as substrate temperature [19], stabilizing elements [20], composition [14], and stress [21], which in turn affect the magnetic properties of the CoPt-based media. Since the former three conditions are kept constant in our work, we suspect that by inserting a few nanometers thick CoPt layer, the stress in the grain is altered. Stress may arise from the difference in the thermal expansion coefficients, or lattice mismatch between the layers [21]. In our work, we inserted the CoPt as underlayer of CoCrPt, the lattice mismatch can be reduced, compared with using Ru as the conventional underlayer. From Figures 3 (b-e), the measured *d*-spacing of $Ru(0\bar{1}10)_{hcp}$, $CoPt(0\bar{1}11)_{hcp}$, $CoCrPt(002)_{fcc}$, $CoCrPt(0\bar{1}11)_{hcp}$ planes are around 0.235 nm, 0.210 nm, 0.188 nm, and 0.201 nm, respectively, which indicates a reduction in the difference of lattice constant from Ru_{hcp} underlayer to $CoCrPt_{hcp}$. This could be the reason why much less stacking faults can be found in the media sample with 3 nm CoPt inserting layer in constrast to the samples with 6 nm CoPt, where the measured *d*-spacing of $CoPt(002)_{fcc}$ and $CoCrPt(002)_{fcc}$ are both about 0.196 nm, indicating a larger strain at the $CoCrPt_{fcc}/CoCrPt_{hcp}$ interface by comparing with the value of 0.188 nm of $CoCrPt(002)_{fcc}$. The change in the lattice constant in $CoCrPt_{fcc}$ can be attributed to strain relaxation as film grows thicker.

As illustrated earlier, the highest H_c and H_n of our media sample with 3 nm CoPt insertion layer can be attributed to lowest amount of stacking faults and fcc phase found in the CoCrPt grain. Both $CoPt_{hcp}$ and $CoCrPt_{hcp}$ contributed to this high H_c and H_n compared with conventional granular media (due to increase of K_u and V). With further increase in the CoPt thickness, the amount of stacking faults in CoCrPt grain increases, accompanied with an increase of fcc phase in both CoPt and CoCrPt layers. The fcc phase with much lower anisotropy has limited contribution to the overall anisotropy of the media stack and as a result, the anisotropy of the grains decrease with thicker CoPt layers.

IV. CONCLUSION

In summary, we have studied the microstructural properties of perpendicular media sample by inserting a near-equiatomic CoPt layer between the CoCrPt and Ru layers. We found that CoPt initially grows in the hcp phase and slowly transforms to fcc phase as the thickness increases. The number of stacking faults increases with the presence of $CoPt_{fcc}$. HRTEM measurements showed that the amount of stacking fault per grain is proportional to the thickness of CoPt. With further increase in the CoPt thickness from 3 nm to 4.5 and 6 nm, H_c and H_n were reduced. We attribute this deterioration in magnetic properties to the increase in stacking faults per grain and higher content of fcc phase, which have a lower anisotropy in both CoPt and CoCrPt.

REFERENCES

[1] S.N. Piramanayagam, J. Appl. Phys., vol. 102, 011301, (2007).
[2] S. N. Piramanayagam, J.Z. Shi, H.B. Zhao, C.S. Mah, J. Zhang, IEEE Trans. Magn. 41(10), 3190 (2005).
[3] R. Victora, and X. Shen, IEEE Trans. Magn. 41, 537 (2005).
[4] D. Suess, J. Lee, J. Fidler, H. S. Jung, E. M. T. Velu, W.Jiang, S. S. Malhotra, G. Bertero, and T. Schrefl, IEEE Trans. Magn. 45, 88 (2009).
[5] B. Ma, H. Wang, H. Zhao, C. Sun, B.R. Acharya, and J.-P. Wang, J. Appl. Phys. 109, 083907 (2011).
[6] J.G. Zhu and Y.M. Wang, IEEE Trans. Magn. 47 (10) 4066-4072 (2011).
[7] N. Gaur, K.K.M. Pandey, S.L. Maurer, S.N. Piramanayagam, R.W. Nunes, H. Yang, and C. S. Bhatia, J. Appl. Phys., 110, 083917 (2011)
[8] H.S. Jung, M. Kuo, S.S. Malhotra and G. Bertero, Appl. Phys. Lett. 91, 212502 (2007).
[9] V. Parasote, M.C. Cadeville, G. Garreau, E. Beaurepaire, Journal of Magnetism and Magnetic Materials 198-199 375-377 (1999)
[10] A-C. Sun, F-T. Yuan, J-H. Hsu, and H.Y. Lee, Scripta Materialia 61 713–716 (2009).
[11] T. Shimatsu, H. Sato,K. Mitsuzuka, H. Kataoka, H. Aoi, S. Okamoto, O. Kitakami, J. Appl. Phys. 105, 07C109 (2009);
[12] H. Yuan, and D.E. Laughlin, J. Appl. Phys. 105, 07A712, (2009).
[13] S.N. Piramanayagam and K. Srinivasan, Appl. Phys. Lett., 91(14) 142508 (2007).
[14] T. Kubo, Y. Kuboki, M. Ohsawa, R. Tanuma, A. Saito, T. Oikawa, H. Uwazumi, and T. Shimatsu, J. Appl. Phys. 97, 10R510 (2005).
[15] T. Shimatsu, H. Sato, T. Oikawa, Y. Inaba, O. Kitakami, S. Okamoto, H. Aoi, H. Muraoka, and Y. Nakamura, IEEE Trans. Magn. 41, 566 (2005).
[16] B. Varghese, S.N. Piramanayagam, Y. Yang, S.K. Wong, H.K. Tan and I. Okamoto, J. Appl. Phys., 115, 17B707 (2014).
[17] J. Johansson, L. S. Karlsson, C. P. T. Svensson, T. Martensson, B. A. Wacaser, K. Deppert, L. Samuelson, and W. Seifert, Nat. Mater. 5, 574 (2006).
[18] Y. Yang, B. Varghese, H.K. Tan, S.K. Wong, and S.N. Piramanayagam, J. Appl. Phys., 115, 083910 (2014).

[19] Y. Shen, B. Y. Wong, and D. E. Laughlin, J. Appl. Phys. 76, 8174 (1994).
[20] Y. Yu, J. Shi and Y. Nakamura, IEEE Trans. Magn. 46, 1663 (2010).
[21] T. P. Nolan, R. Sinclair, R. Ranjan, T. Yamashita, J. Appl. Phys. 73, 5566 (1993).

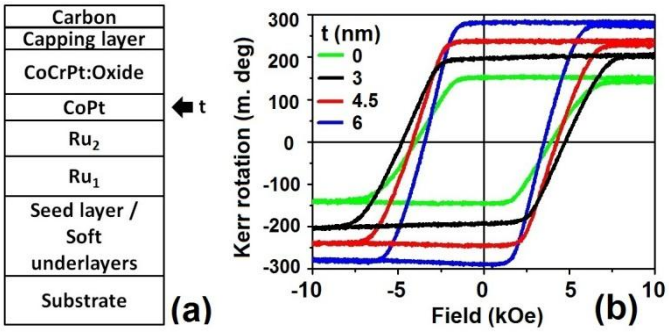

Fig. 1(a). Schematic of the layer structure of the recording media fabricated for this study and (b) Hysteresis loops of the samples with different thickness of CoPt layers, as measured using MOKE.

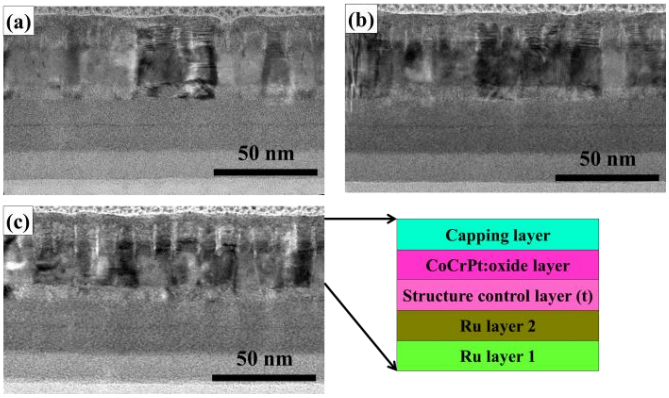

Fig. 2. Low magnification cross-sectional TEM images of recording media samples with CoPt thickness varied from (a) 3nm, (b) 4.5 nm, and (c) 6 nm. The CoCrPt, CoPt, and Ru layers are indicated in (c).

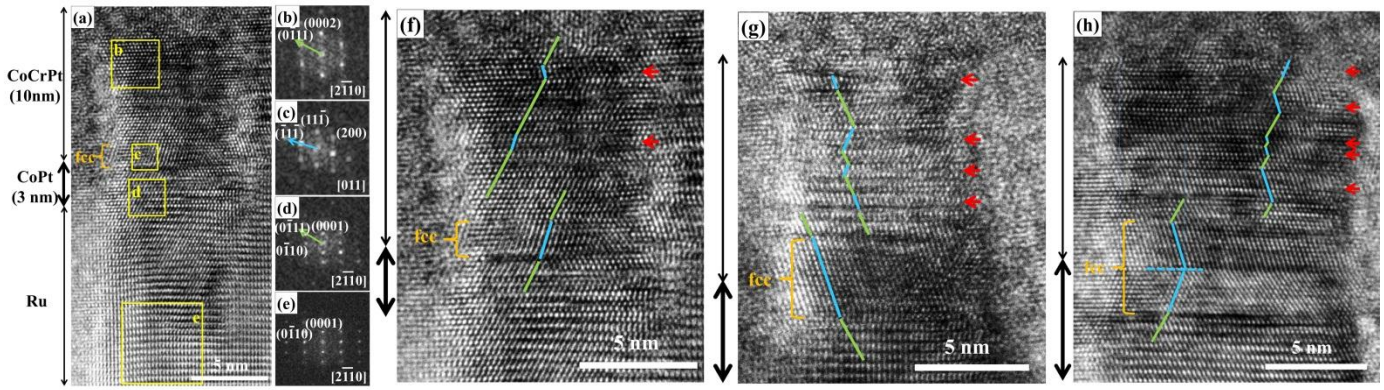

Fig. 3 [Two column] TEM images of samples with thickness of CoPt layers (a,f) 3 nm, (g) 4.5 nm and (h) 6 nm. (b-e) are the FFT of the layers selected by white box in (a), corresponding to Ru, $CoPt_{hcp}$, $CoCrPt_{fcc}/CoPt_{fcc}$, and top $CoCrPt_{hcp}$ phases. The phase transformation at the CoPt/CoCrPt interface and in the CoCrPt grain is indicated by $(\bar{1}1\bar{1})_{fcc}$ (blue lines) and $(0\bar{1}11)_{hcp}$ planes (green lines). The stacking faults in CoCrPt grain are indicated by red arrows in (a, f, g and h).

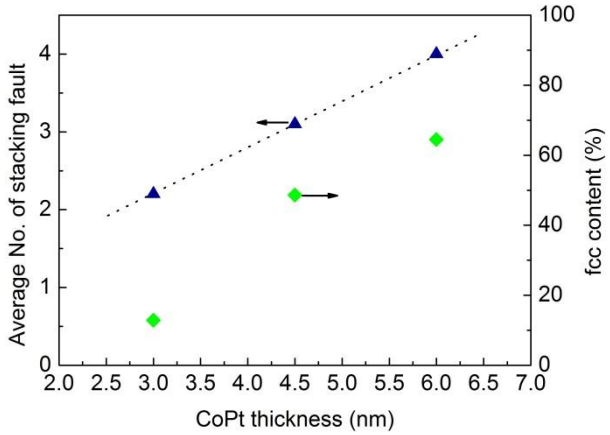

Fig. 4. Plot of fcc content (%) and the average number of stacking fault per grain as a function of CoPt thickness.